Transgenerational sterility of small RNA genome silencing mutants in response to germ granule dysfunction

Katherine Kretovich Billmyre[1,2]*, Bree Heestand[1,2,3]*, Maya Spichal[1,2]* and Shawn Ahmed[1,2,3]

[1]Department of Genetics, University of North Carolina, Chapel Hill, NC, USA
[2]Department of Biology, University of North Carolina, Chapel Hill, NC, USA
[3]Lineberger Comprehensive Cancer Center, University of North Carolina, Chapel Hill, NC, USA
To whom correspondence should be addressed. E-mail: shawn@med.unc.edu

* These authors contributed equally to this manuscript

Abstract

Deficiency for small RNA nuclear silencing proteins that promote heterochromatin maintenance leads to defects in germ cell immortality where fertile mutant strains become sterile over successive generations. The transgenerational sterility of small RNA nuclear silencing is associated with mis-wiring of small RNA pathways and with progressive deterioration of heterochromatin, which leads to increased levels of transposon expression, transposition and RNA-DNA hybrids. However, the cause of transgenerational sterility in small RNA nuclear silencing mutants is not understood. We found that sterile small RNA genome silencing mutants display altered perinuclear germ granules. Moreover, germ granule dysfunction was sufficient to induce phenotypes associated with sterile small RNA genome silencing mutants, including germline atrophy, reproductive diapause and univalents in oocytes. We conclude that germ granules, which are intimately associated with small RNA nuclear silencing proteins and RNAs, orchestrate the transgenerational sterility of small RNA genome silencing mutants.

Introduction

Germ cells give rise to the mortal somatic tissue while maintaining themselves in a pristine condition that allows them to be propagated for indefinite number of generations. This capacity for self-renewal is termed “germ cell immortality”, and functions to protect the germline from stressors which can result in sterility[1]. *C. elegans* mutations in genes that promote small RNA-mediated genome silencing (Fig. 4a) can cause a Mortal Germline *(mrt)* phenotype, where fertility occurs for several generations but leads to a deterioration of fertility in late-generations

51 and finally to complete sterility. Many *mrt* mutants exhibit a conditional transgenerational
52 sterility phenotype, such that they only become sterile when grown at the non-permissive
53 temperature 25˚C[1]. Examples of conditional *mrt* mutants include a nuclear RNAi defective
54 mutant, *nrde-2,* a number of heritable RNAi mutants, including *hrde-1*, and two RNAi defective
55 mutants, *rsd-2* and *rsd-6*[2–7]. Other *mrt* mutants display progressive sterility at any temperature,
56 including *prg-1*/piRNA mutants and nuclear RNAi mutants *nrde-1* and *nrde-4*[4–6,8–10].
57
58 Piwi is a conserved germ line Argonaute protein that interacts with thousands of small RNAs
59 termed piRNAs to repress transposons and foreign nucleic acids that represent parasitic threats
60 to the integrity of the genome. Deficiency for the *C. elegans* Piwi ortholog *prg-1* was recently
61 shown to elicit a striking germ cell atrophy phenotype at the generation of sterility, as L4 larvae
62 mature into 1 day old adults[11]. Moreover, atrophied germ lines of sterile *prg-1* mutants can
63 regrow on day 2 of adulthood, and a small fraction of sterile adults can become fertile again if
64 animals are shifted to a distinct food source[11]. This indicates that the late-generation sterility of
65 *prg-1*/Piwi mutants is a form of reproductive arrest termed Adult Reproductive Diapause[12].
66 Temperature-sensitive small RNA genome silencing mutants *rsd-2* and *rsd-6* also exhibit small
67 and empty germlines at the generation of sterility, indicating that the transgenerational sterility
68 of small RNA genome silencing mutants elicits consistent developmental consequences[2].
69 Although these *mrt* mutants likely suffer from transgenerational deterioration of
70 heterochromatin, the underlying cause of the late-generation sterility of these mutants is not
71 understood.
72

73 The fertility defects in response to heterochromatin dysfunction have been associated with
74 increased levels DNA damage[4,13]. Moreover, the fertility of late-generation *prg-1* mutants could
75 be improved by RNAi knockdown of the Mirage transposon, suggesting a link between
76 transposition and fertility defects of *prg-1* mutants[4]. Furthermore, RNA-DNA hybrids that result
77 from collisions between replication forks and RNA polymerase were increased in response to
78 heterochromatin defects[4,13]. *prg-1* mutants display progressively increased levels of germline
79 apoptosis when grown for successive generations, and at the generation of sterility apoptosis
80 promotes germ cell atrophy for *rsd-2*, *rsd-6* and *prg-1* mutants[2,10,11]. At the same time, the
81 frequency of spontaneous mutation in either *prg-1* or *rsd-6 mrt* mutants is minimal[2,7,10].
82 Moreover, temperature shift experiments have indicated that the trigger of the
83 transgenerational fertility defects in such mutants is reversible and therefore not the
84 consequence of (transposon-induced) changes to the genome[7]. Finally, high levels of
85 transposition in *C. elegans mutator* mutants that experience significant levels of transposition
86 do not display progressive sterility phenotype if propagated at low temperatures[10].
87
88 Another possible cause of small RNA mutant germline atrophy is disruption in proper function
89 of the pro- and anti-silencing of the *C. elegans* genome [14,15]. Major proteins involved in these
90 pathways such as PRG-1 and CSR-1, respectively, are located in perinuclear germ granules,
91 which are conserved germline structures that consist of liquid droplets that interact with
92 nuclear pore complexes (NPCs) and are necessary for fertility [16]. In *C. elegans*, germ granules
93 are termed P-granules based on antibodies that label the P blastomere that generates the germ
94 cell lineage[17].

95 Here we study the late-generation sterility phenotype of small RNA-mediated genome silencing
96 mutants and link this to dysfunction of P granules, which play a central role in modulating the
97 process of small RNA genome silencing itself.
98
99 **Results**
100 **Genome instability in small RNA mutants**
101 Transgenerational sterility in *C. elegans* telomerase mutants that lack the ability to maintain
102 sequences that cap chromosome ends is caused by high levels of telomere fusions and
103 associated damage to chromosome termini[18]. We examined *prg-1* mutants grown at 20°C at
104 progressive generations for the presence of the DNA damage response and observed that late-
105 generation *prg-1* mutants and sterile *prg-1* mutants showed a significant 3 to 6 fold
106 upregulation of DNA damage response when compared to wild-type controls or to early
107 generation *prg-1* mutants (Fig. 1a). However, the number of cells with DNA damage was not
108 consistently increased in sterile *prg-1* mutant samples, when compared to fertile, late-
109 generation controls (Fig. 1a). We also tested levels of DNA damage response in the
110 temperature-sensitive small RNA mutants *rsd-6, nrde-2* and *hrde-1*. We found that the wild-
111 type control DNA damage response was upregulated in many cells at 25°C but that this level did
112 not change in sterile *rsd-6, nrde-2* or *hrde-1* mutant germlines sterile *prg-1* (Fig. 1b). Therefore,
113 although the DNA damage response is transgenerationally upregulated in *prg-1* mutants, it is
114 unlikely to be the cause of sterility in small RNA genome silencing mutants.
115
116 **Small RNA mutants exhibit P-granule defects at sterility**

117 Whilst we were characterizing the germ line defects present sterile *rsd-6* small RNA genomic
118 silencing mutants in immunofluorescence assays, we happened to use an antibody against P-
119 granules as a positive control. Surprisingly, we found there was an altered P-granule staining
120 pattern when compared to fertile r*sd-6* mutant siblings. This finding was interesting as PRG-1
121 localizes to P-granules and deficiency for PRG-1 causes delocalization of the structural P-granule
122 protein PGL-1[19]. Additionally, combined loss of the epigenomic regulators SPR-5 and LET-418
123 results in immediate sterility that is associated with germ cell to soma transformation that
124 disrupts P granule structures, and the H3K9 methylation modifier SET-2 can cause a loss of
125 perinuclear P-granules in a context where the nuclear RNAi pathway acts in parallel to promote
126 germ cell identity[20,21]. We therefore asked if sterility in small RNA genomic mutants was
127 consistently linked with P-granule dysfunction by testing sterile small RNA mutants *hrde-1*, *rsd-*
128 *6,* and *nrde-2* and found that sterile animals display P-granule dysfunction, but that P-granule
129 defects were absent or comparatively minor in fertile late-generation animals that were close
130 to the generation of sterility (Fig. 2c-d, S1, Table 1). When compared to wild-type controls, P-
131 granule dysfunction in the sterile mutants ranged from a loss of P-granules in a subset of cells
132 to varying amounts of P-granule disorganization (Fig. 2c-d). Sterile *hrde-1* mutant animals
133 displayed the most severe P-granule phenotype, as the majority of sterile *hrde-1* mutant germ
134 cells exhibited little to no staining (Fig. S1).
135 Large-scale apoptosis occurs in some but not all *prg-1* mutants as L4 larvae to adult
136 transition at generation of sterility[11], and P-granules have been shown to vanish in cells that
137 undergo apoptosis[22,23]. However, we saw widespread P granule dysfunction in sterile germlines
138 of *rsd-6* mutants that were wildtype in size and had not undergone significant levels of

139 apoptosis (Fig. 2d). Moreover, sterile *nrde-4* mutant germlines did not show obvious defects to
140 the structure of P-granules, indicating that the sterility of small RNA genome silencing mutants
141 is not always associated with overt effects on P granule structure (Fig. S1).
142 In contrast to many small RNA genome silencing mutants where fertility defects are not
143 severe until the generation of sterility, late-generation *prg-1* mutants display very small brood
144 sizes prior to sterility[4,11]. By immunofluorescence, late-generation *prg-1* mutants had a wide
145 range of P-granule defects that could be identified in fertile and sterile animals (Fig. 2b, S1).
146 Many germlines exhibited strong P-granule dysfunction that either resulted in a total absence
147 of P-granules or irregular distribution (Fig. 2b, S1). Often these strong P-granule defects
148 coincided with sterile animals, though some sterile *prg-1* germlines displayed mild defects.
149
150 We next examined a temperature sensitive mutant, *rbr-2(tm1231)*, which encodes a histone 3
151 lysine 4 demethylase known to promote genomic silencing and is thought to function
152 downstream of small RNAs to promote genomic silencing[24]. Sterile *rbr-2* animals displayed loss
153 of P-granules in many germ cells, but late-generation fertile *rbr-2* animals did not exhibit
154 obvious P-granule defects (Fig. 2e).
155
156 *C. elegans* P-granules are adjacent to Mutator bodies[28], where small RNA-mediated silencing
157 pathway proteins function to amplify primary siRNA populations into effector secondary
158 siRNAs. *mutator* mutants are dysfunctional for RDRP-mediated biogenesis of effector small RNA
159 and although they remain fertile indefinitely at low temperatures, they display an immediate

160 highly penetrant sterility phenotype at 25°C that could be caused by dysfunction of small RNA-
161 mediated heterochromatin.
162
163 **P-granule dysfunction is sufficient to elicit phenotypes of sterile small RNA silencing mutants**
164 Given that P-granule loss has been shown to cause a germline to soma transformation in
165 conjunction with short germlines in adults [25,26], we assessed the consequences of an RNA
166 interference clone, that simultaneously targets four P-granule subunits *pgl-1*, *pgl-3*, *glh-1*, *glh-4*
167 [25,26]. Knockdown of P-granules by RNAi resulted in F2 sterile animals at 25˚C (80%) (Fig. 3a).
168 When *prg-1* mutants became sterile their germline profile shifts specifically at adulthood from
169 large L4 larval stage germlines to adult only atrophy[11]. Interestingly, sterile P-granule RNAi F2
170 adults at 25˚C displayed a range of germline phenotypes similar to those observed in our small
171 RNA silencing sterile adults[11] (Fig. 3b).
172 To confirm that the apparent germline degeneration phenotypes of P-granule depleted
173 adults were not due to failure of germ cells to proliferate in early development, we collected L4
174 larval stage F2 animals and assessed germline development. The germlines of F2 P-granule RNAi
175 L4 larvae were normal in size in comparison to control worms, but a significant change in their
176 germline profile occurred as these animals matured into adults with pronounced germ cell
177 atrophy occurring at adulthood (Fig. 3b, p=3.93e-24). Furthermore, for sterile P-granule
178 depleted worms that contained oocytes, 45.5% of oocytes contained 7-12 univalents (Fig. 3c, e-
179 h), revealing a phenocopy of the oocyte univalents that was previously observed for oocytes of
180 late-generation sterile *rsd-6, hrde-1* and *nrde-2* mutants[2].
181

182 ***prg-1* mutants phenocopy and *pgl-1* mutants**

183 If P-granule defects cause the late-generation sterility of small RNA genome silencing mutants,
184 we hypothesized that the germline atrophy phenotypes observed in P-granule knockdown
185 worms might have the potential to mimic the delayed fertility phenomenon for sterile *prg-1*
186 mutant adults, which can regrow atrophied germlines to become fertile[11]. We therefore used
187 the temperature-sensitivity sterility of *pgl-1* mutants that become sterile in the F1 generation
188 at 25˚C but can be fertile at low temperatures. While most F1 *pgl-1* animals at 25˚C displayed
189 normal germlines at the L4 larval stage, there was a significant shift in the germline profiles
190 with 52% of day 1 adults showing germline atrophy (Fig. 3b, p=1.04E-35), similar to P-granule
191 RNAi knockdown and sterile *prg-1* mutants[11]. Furthermore, when these sterile *pgl-1* worms
192 were scored for univalents in worms that contained oocytes, we found that 56.7% of oocytes
193 had univalents, in agreement with the oocyte univalent observed for P-granule RNAi oocytes
194 (Fig. 3c). 20% of F1 *pgl-1* mutants gave rise to maternally depleted P-granule F2 animals and
195 these were uniformly sterile. F2 L4 larval stage germline profiles displayed more severe germ
196 cell proliferation defects than the L4 F1 generation, and day 1 adults showed a striking 54%
197 increase in empty germlines (Fig. 3d). This suggest that F1 generation *pgl-1* mutants mimic the
198 germ cell degeneration phenotypes of sterile small RNA genome silencing mutants at the L4 to
199 adult transition, whereas maternal depletion of *pgl-1* elicits more pronounced effects on germ
200 cell proliferation at earlier stages of development and at the L4/adult transition.

201

202 When sterile F1 *pgl-1* day 1 adults were shifted to 20˚C, some animals were capable of
203 regrowing their germlines. We scored the germline profiles of sterile F1 *pgl-1* adults shifted to

204 20°C after 48 hours and saw a significant change compared to controls (Fig. 3i, p=0.007). The
205 germline profile shifted from a high incidence of atrophy germlines towards an increase in large
206 germlines when compared to sterile F1 *pgl-1* sibling controls that remained at 25°C (Fig. 3i). In
207 agreement with this data, several days after 1 day old sterile F1 *pgl-1* mutant adults at 25°C
208 were shifted to 20°C, we observed that some laid oocytes and dead embryos and rarely
209 progeny, whereas sterile day 1 *pgl-1* at 25°C never gave rise to oocytes, dead embryos or
210 progeny (Fig. 3j). The frequency of fertility in this circumstance is very similar to that of 5 day
211 old sterile *prg-1* mutant adults that exit Adult Reproductive Diapause in response to an altered
212 food source[11]. These results indicate that severe P-granule dysfunction and associated sterility
213 can mimic a state of reproductive quiescence that does not abolish fertility.
214
215 **Discussion**
216 Previous work has established that a subset of small RNA genome silencing mutants display a
217 transgenerational sterility phenotype in conjunction with desilencing of various repetitive
218 segments of the genome[2,6,10]. However, the molecular mechanism that evokes
219 transgenerational sterility has remained an open question. We show that *prg-1* and several
220 other small RNA mutants show P-granule defects at sterility[27]. Given that these mutants
221 experience desilencing of heterochromatic transposons, their sterility might occur in response
222 to an increased DNA damage response induced by transposition or by R-loop formation.
223 However, we observed that sterile late-generation small RNA mutants at 25°C displayed similar
224 levels of DNA damage response as wild-type controls. Consistently, while levels of DNA damage

225 increased in late-generation *prg-1* mutants, these levels did not consistently increase at
226 sterility.
227
228 We examined the integrity of P-granules in sterile small RNA genome silencing mutants and
229 found that P-granule defects occur in sterile animals of most late-generation *mortal germline*
230 mutants examined. Our data further show that a direct knockdown of P-granules by RNAi was
231 sufficient to mimic the germline atrophy and meiotic recombination defects that are observed
232 for small RNA mutants. The similarities between the sterility phenotypes of *pgl-1* mutants, P-
233 granule RNAi treated animals and small RNA silencing mutants imply that P-granule defects are
234 likely to cause sterility in small RNA mutants. Furthermore, our data indicate that univalent
235 chromosomes that are observed in oocytes of some sterile small RNA genome silencing animals
236 are a likely secondary consequence of P-granule dysfunction that indirectly disrupts a process
237 that promotes meiotic recombination[29,30]. Interestingly, when *pgl-1* mutants were shifted to
238 the permissive temperature of 20°C, there is a decrease in empty and atrophied germlines, a
239 corresponding increase in the number of large germlines and a few give rise to progeny. These
240 results closely resemble the regrowth of the germline and the fertility observed for sterile late-
241 generations *prg-1* mutants that are in Adult Reproductive Diapause[11]. Taken together our
242 results suggest that P-granule dysfunction is likely to be the mechanism that promotes the
243 reproductive arrest phenotype termed Adult Reproductive Diapause.
244
245 Small RNA silencing proteins such as CSR-1, PRG-1 or HRDE-1 are localized to P-granules, and it
246 has been hypothesized that small RNA dysfunction in P-granules could be the cause of sterility

247 in small RNA genome silencing mutants[14,19]. Our evidence supports a loss of P-granule structure
248 and function, not DNA damage response, as the trigger of sterility in late-generation *mrt*
249 mutants (Fig. 4b). Our results establish a novel framework to consider inheritance in the
250 context of epigenetic stress and how this can evoke transgenerational sterility. Future efforts to
251 understand how epigenomic defects lead to P-granule mis-regulation may provide insight into
252 the precise cause of sterility in small RNA silencing mutants. We suggest that the sterility in
253 response to epigenome dysfunction is consistent with a developmental arrest mechanism to
254 protect the genome or epigenome in times of stress. We note that transposons and viruses that
255 are central targets of the small RNA genome silencing system are likely in a continuous arms
256 race between parasite and host, where components of P-granules are likely to be targeted[27]. It
257 is therefore reasonable to hypothesize and arrest mechanism in the context of an attack on the
258 P-granule silencing system, which is predicated on the integrity of the P-granules themselves.
259
260
261 **Methods**
262 **Strains:**
263 All strains were cultured at 20°C or 25°C on Nematode Growth Medium (NGM) plates seeded
264 with *E. coli* OP50. Strains used include Bristol N2 wild type, *hrde-1(tm1200) III, rsd-6(yp11) I,*
265 *nrde-2(gg95) II,* and *rbr-2(tm1231) IV.*
266
267 **RNAi Assay:**

268 Feeding RNAi plates harboring host bacteria HT115(DE3) engineered to express "quad" dsRNA
269 (targeting P-granules) were obtained from Susan Strome [25,26]. L1 larvae were placed onto
270 freshly prepared feeding RNAi plates with dsRNA induced by 1 mM IPTG (isopropyl-β-D(-)-
271 thiogalactopyranoside) and were transferred after 1 generation at 25°C and collected at F2
272 adults as described in Knutson et al., 2017 for DAPI staining, oocyte and germline analysis.
273
274 **DAPI staining and Scoring:**
275 DAPI staining was performed as previously described[18]. Briefly, L4 larvae were selected from
276 sibling plates and sterile adults were singled as late L4s, observed 24 hours later for confirmed
277 sterility, and then stained 48 hours after collection. Univalents were scored by counting DAPI
278 bodies in the -1 to -4 oocytes. Germline profiles were scored using the method outlined in
279 Heestand et al 2018.
280
281 **Statistical Analysis**
282 Statistical analysis was performed as previously described[11]. Briefly, statistical analysis was
283 performed using the R statistical environment[31]. For germline phenotypes, contingency tables
284 were constructed and pairwise Chi Square tests with Bonferroni correction was used to
285 determine significant differences in in germline phenotype distributions.
286
287 **Immunofluorescence:**
288 Adult hermaphrodites raised at 20°C or 25°C were dissected in M9 buffer and flash frozen on
289 dry ice before fixation for 1 min in methanol at -20°C. After washing in PBS supplemented with

290 0.1% Tween-20 (PBST), primary antibody diluted in in PBST was used to immunostain overnight
291 at 4 °C in a humid chamber. Primaries used were 1:50 OIC1D4 (Developmental Studies
292 Hybridoma Bank). Secondary antibody staining was performed by using an Cy3 donkey anti-
293 mouse or Cy-5 donkey anti-rabbit overnight at 4°C. All images were obtained using a LSM 710
294 laser scanning confocal and were taken using same settings as control samples. Images
295 processed using ImageJ.
296
297 **DNA Damage Assay:**
298 Worms that were close to sterility were isolated and defined as sterile if they did not have any
299 offspring as day 2 adults at 25˚C. The presence of the DNA damage response by using a
300 phospho-specific antibody targeting the phosphorylated consensus target site of ATM and ATR
301 kinases (pS/TQ). This antibody has only been shown to stain a DNA damage response in the
302 germline[32].
303
304 **Scoring of P-granules:**
305 The number of P-granules was determined in 60 representative DAPI-stained nuclei of the
306 middle section of a z-stack taken at 40x for 3 different germlines per condition. P-granule
307 counts were attributed to different number counts per nucleus (0, 1-4, 5-8, >8).
308
309 Author Contributions
310 KB, MS and BH performed experiments. KB, MS, BH and SA wrote manuscript.
311

312

313 References

314 1. Smelick, C. & Ahmed, S. Achieving immortality in the C. elegans germline. *Ageing Res.*

315 *Rev.* **4,** 67–82 (2005).

316 2. Sakaguchi, A. *et al.* Caenorhabditis elegans RSD-2 and RSD-6 promote germ cell

317 immortality by maintaining small interfering RNA populations. *Proc. Natl. Acad. Sci. U. S.*

318 *A.* **111,** E4323-31 (2014).

319 3. Ashe, A. *et al.* piRNAs can trigger a multigenerational epigenetic memory in the germline

320 of C. elegans. *Cell* **150,** 88–99 (2012).

321 4. McMurchy, A. N. *et al.* A team of heterochromatin factors collaborates with small RNA

322 pathways to combat repetitive elements and germline stress. *Elife* **6,** (2017).

323 5. Buckley, B. A. *et al.* A nuclear Argonaute promotes multigenerational epigenetic

324 inheritance and germline immortality. *Nature* **489,** 447–451 (2012).

325 6. Burkhart, K. B. *et al.* A pre-mRNA-associating factor links endogenous siRNAs to

326 chromatin regulation. *PLoS Genet.* **7,** e1002249 (2011).

327 7. Spracklin, G. *et al.* Identification and Characterization of Caenorhabditis elegans RNAi

328 Inheritance Machinery. *Genetics* (2017).

329 8. Batista, P. J. *et al.* PRG-1 and 21U-RNAs interact to form the piRNA complex required for

330 fertility in C. elegans. *Mol. Cell* **31,** 67–78 (2008).

331 9. Das, P. P. *et al.* Piwi and piRNAs Act Upstream of an Endogenous siRNA Pathway to

332 Suppress Tc3 Transposon Mobility in the Caenorhabditis elegans Germline. *Mol. Cell* **31,**

333 79–90 (2008).

334 10. Simon, M. *et al.* Reduced insulin/IGF-1 signaling restores germ cell immortality to
335 Caenorhabditis elegans Piwi mutants. *Cell Rep.* **7,** 762–73 (2014).
336 11. Heestand, B., Simon, M., Frenk, S., Titov, D. & Ahmed, S. Transgenerational sterility of
337 Piwi mutants represents a dynamic form of Adult Reproductive Diapause. *Cell Rep.* **in**
338 **press,** (2018).
339 12. Angelo, G. & Van Gilst, M. R. Starvation Protects Germline Stem Cells and Extends
340 Reproductive Longevity in C. elegans. *Science (80-.).* **326,** 954–958 (2009).
341 13. Zeller, P. *et al.* Histone H3K9 methylation is dispensable for Caenorhabditis elegans
342 development but suppresses RNA:DNA hybrid-associated repeat instability. *Nat. Genet.*
343 **48,** 1385–1395 (2016).
344 14. de Albuquerque, B. F. M., Placentino, M. & Ketting, R. F. Maternal piRNAs Are Essential
345 for Germline Development following De Novo Establishment of Endo-siRNAs in
346 Caenorhabditis elegans. *Dev. Cell* **34,** 448–56 (2015).
347 15. Phillips, C. M., Brown, K. C., Montgomery, B. E., Ruvkun, G. & Montgomery, T. A. piRNAs
348 and piRNA-Dependent siRNAs Protect Conserved and Essential C. elegans Genes from
349 Misrouting into the RNAi Pathway. *Dev. Cell* **34,** 457–465 (2015).
350 16. Updike, D. L., Hachey, S. J., Kreher, J. & Strome, S. P granules extend the nuclear pore
351 complex environment in the *C. elegans* germ line. *J. Cell Biol.* **192,** 939–948 (2011).
352 17. Strome, S. & Wood, W. B. Immunofluorescence visualization of germ-line-specific
353 cytoplasmic granules in embryos, larvae, and adults of Caenorhabditis elegans. *Proc.*
354 *Natl. Acad. Sci. U. S. A.* **79,** 1558–62 (1982).
355 18. Ahmed, S. & Hodgkin, J. MRT-2 checkpoint protein is required for germline immortality

356 and telomere replication in C. elegans. *Nature* **403,** 159–64 (2000).

357 19. Phillips, C. M., Brown, K. C., Montgomery, B. E., Ruvkun, G. & Montgomery, T. A. piRNAs
358 1. Phillips, C. M., Brown, K. C., Montgomery, B. E., Ruvkun, G. & Montgomery, T. A.
359 piRNAs and piRNA-Dependent siRNAs Protect Conserved and Essential C. elegans Genes
360 from Misrouting into the RNAi Pathway. Dev. Cell 34, 457–465 (2015).and piRNA-Dep.
361 *Dev. Cell* **34,** 457–465 (2015).

362 20. Käser-Pébernard, S., Müller, F. & Wicky, C. LET-418/Mi2 and SPR-5/LSD1 cooperatively
363 prevent somatic reprogramming of C. elegans germline stem cells. *Stem cell reports* **2,**
364 547–59 (2014).

365 21. Robert, V. J. *et al. The SET-2/SET1 Histone H3K4 Methyltransferase Maintains*
366 *Pluripotency in the Caenorhabditis elegans Germline*. *Cell Reports* **9,** (2014).

367 22. Sung, M., Kawasaki, I. & Shim, Y.-H. Depletion of *cdc-25.3* , a *Caenorhabditis elegans*
368 orthologue of *cdc25* , increases physiological germline apoptosis. *FEBS Lett.* **591,** 2131–
369 2146 (2017).

370 23. Min, H., Shim, Y.-H. & Kawasaki, I. Loss of PGL-1 and PGL-3, members of a family of
371 constitutive germ-granule components, promotes germline apoptosis in C. elegans. *J. Cell*
372 *Sci.* **129,** 341–353 (2016).

373 24. Alvares, S. M., Mayberry, G. A., Joyner, E. Y., Lakowski, B. & Ahmed, S. H3K4 demethylase
374 activities repress proliferative and postmitotic aging. *Aging Cell* **13,** 245–253 (2014).

375 25. Knutson, A. K. K., Egelhofer, T., Rechtsteiner, A. & Strome, S. Germ Granules Prevent
376 Accumulation of Somatic Transcripts in the Adult Caenorhabditis elegans Germline.
377 *Genetics* **206,** (2017).

378 26. Updike, D. L., Knutson, A. K., Egelhofer, T. A., Campbell, A. C. & Strome, S. Germ-Granule
379 Components Prevent Somatic Development in the C. elegans Germline. *Curr. Biol.* **24,**
380 970–975 (2014).
381 27. Updike, D. & Strome, S. P Granule Assembly and Function in Caenorhabditis elegans
382 Germ Cells. *J. Androl.* **31,** 53–60 (2010).
383 28. Phillips, C. M., Montgomery, T. A., Breen, P. C. & Ruvkun, G. MUT-16 promotes formation
384 of perinuclear mutator foci required for RNA silencing in the C. elegans germline. *Genes*
385 *Dev.* **26,** 1433–44 (2012).
386 29. Loidl, J. Conservation and Variability of Meiosis Across the Eukaryotes. *Annu. Rev. Genet.*
387 **50,** 293–316 (2016).
388 30. Hillers K.J., Jantsch V., Martinez-Perez E. & Yanowitz J.L. in (2017).
389 doi:10.1895/wormbook.1.178.1
390 31. R Core Team. R: A language and environment for statistical computing. *R Foundation for*
391 *Statistical Computing* (2013).
392 32. Vermezovic, J., Stergiou, L., Hengartner, M. O. & d'Adda di Fagagna, F. Differential
393 regulation of DNA damage response activation between somatic and germline cells in
394 Caenorhabditis elegans. *Cell Death Differ.* **19,** 1847–1855 (2012).
395
396 **Figures and Figure Legends**
397
398
399 **Figure 1**

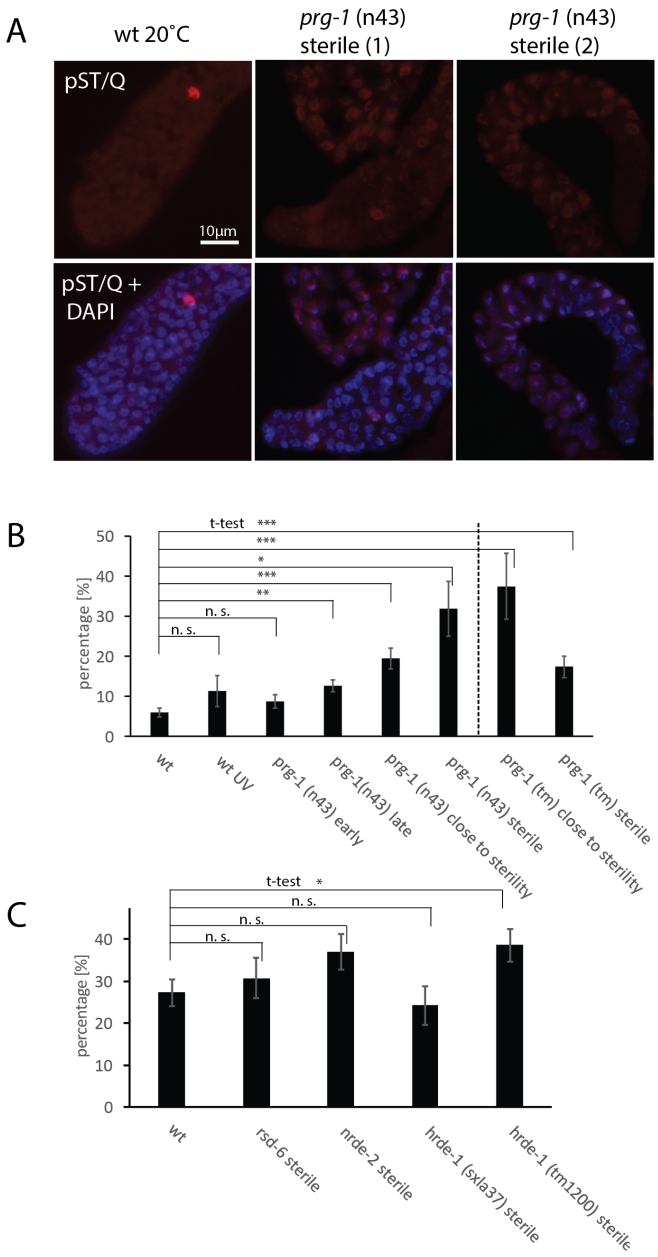

Figure 1: DNA Damage Response is variable in small RNA genome silencing mutants prior to and at sterility. (A) Staining of pS/TQ in wildtype, *prg-1(n43) and prg-1(tm)* mutants. pS/TQ(red) and DAPI(blue) **(B)** Quantification of pS/TQ staining in 20°C wildtype and *prg-1* mutants at different levels of fertility. **(C)** Quantification of pS/TQ staining in 25°C wildtype and small RNA genomic silencing mutants at sterility.

406 **Figure 2**

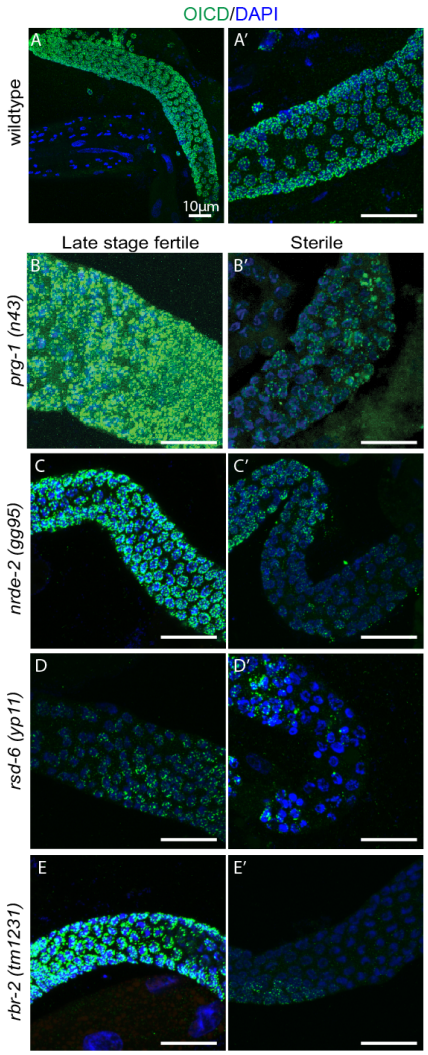

407

408 **Figure 2: At sterility, partial loss of P-granule staining occurred in *prg-1* and temperature-**

409 **sensitive mutants.** Germlines of sterile Day 2-3 adult animals were stained using the OIC1D4

410 antibody against P-granules (green) and DAPI (blue). **(A-A')** Control animals contain uniform

411 puncta of P-granule staining surrounding each nuclei. **(B-E)** Late generation fertile *prg-1, rsd-6*,

412 *nrde-2*, and *rbr-2* animals displayed relatively normal P-granule staining in the germlines. **(B'-E')**

413 *prg-1*, *nrde-2*, *rsd-6* and *rbr-2* sterile animals all exhibited loss of germ cell P-granules. (N=30)

414 Figure 3

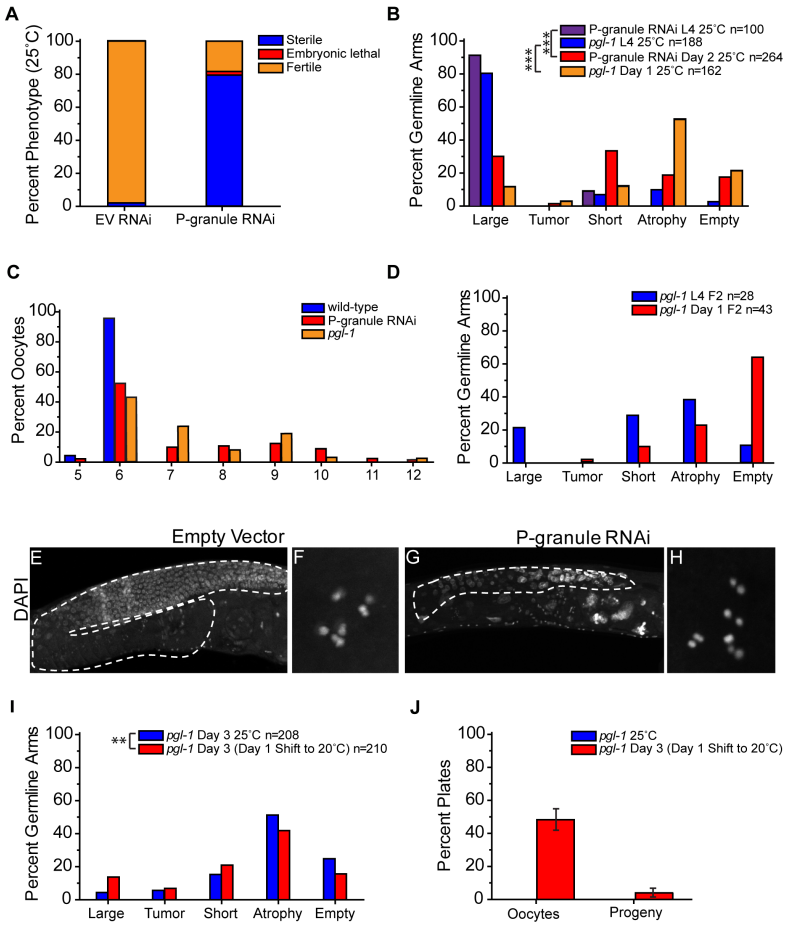

415

416 **Figure 3: Disruption of P-granules by RNAi or loss of *pgl-1* resulted in a similar germline**

417 **atrophy phenotype at 25°C.** (A**)** F2 wild-type (N2) worms on Empty Vector (EV) or P-granule

418 RNAi at 25°C were scored for sterility, embryonic lethality, or fertility. 80% of worms on P-

419 granule RNAi were sterile. (B) F1 L4 *pgl-1* mutants and F2 L4 P-granule RNAi treated animals

420 stained by DAPI contained mostly large germlines while adults exhibited a range of germline

421 phenotypes from empty to large. *** p<0.0001 Fisher's Chi Square test with Bonferroni
422 correction n=total germlines scored **(C)** F1 *pgl-1* mutants and F2 P-granule RNAi treated animals
423 contained oocytes with increased numbers of univalents at sterility as measured by DAPI bodies
424 n=151 wild-type, 81 P-granule RNAi, 37 *pgl-1*. (D) Stained DAPI germlines of sterile F2 L4 *pgl-1*
425 contained a range of germline phenotypes from large to empty. Sterile F2 day 1 *pgl-1* mutants
426 stained by DAPI contained predominantly empty and atrophy germlines. n=total germlines
427 scored. **(E-H)** Representative DAPI images of germline and oocyte defects in empty vector
428 treated animals **(E,F)** and P-granule RNAi treated animals **(G,H)** scale bar=10um. **(I)** *pgl-1* F1
429 worms at 25°C were either DAPI stained as Day 3 adults (blue) or shifted to 20°C at Day 1 and
430 DAPI stained at Day 3 (red) ** p=0.007 Fisher's Chi Square test with Bonferroni correction.
431 n=total germlines scored **(I)** No sterile day 1 *pgl-1* F1 at 25°C laid oocytes or progeny (n=35
432 plates, 350 total worms). Sterile day 1 *pgl-1* shifted to (20°C n=50 plates, 500 worms) gave rise
433 to plates with oocytes and rarely progeny. Plates with oocytes contained both oocytes and
434 dead embryos. Plates with progeny contained embryos that hatched to L1.

435 **Figure 4: Model for P-granule dysfunction in small RNA genome silencing mutants**

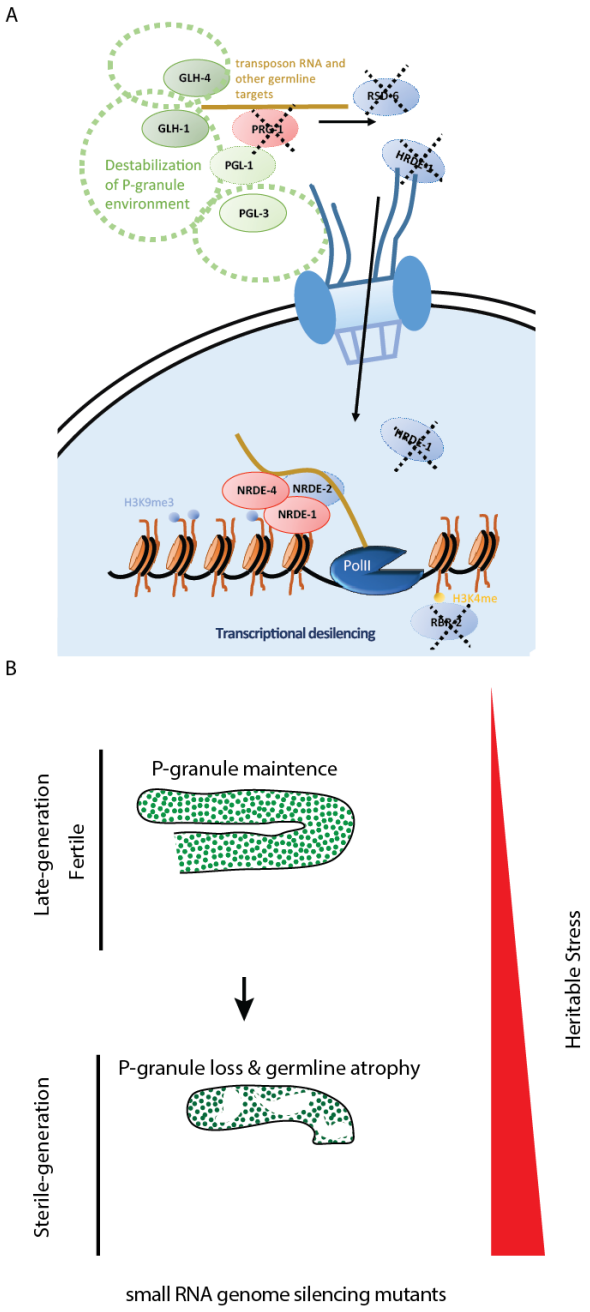

436

437 (A**)** Model for small RNA genome silencing mutants B) Model for accumulating heritable stress

438 in small RNA genome silencing mutants and P-granule function.

439 Supplemental Figure 1

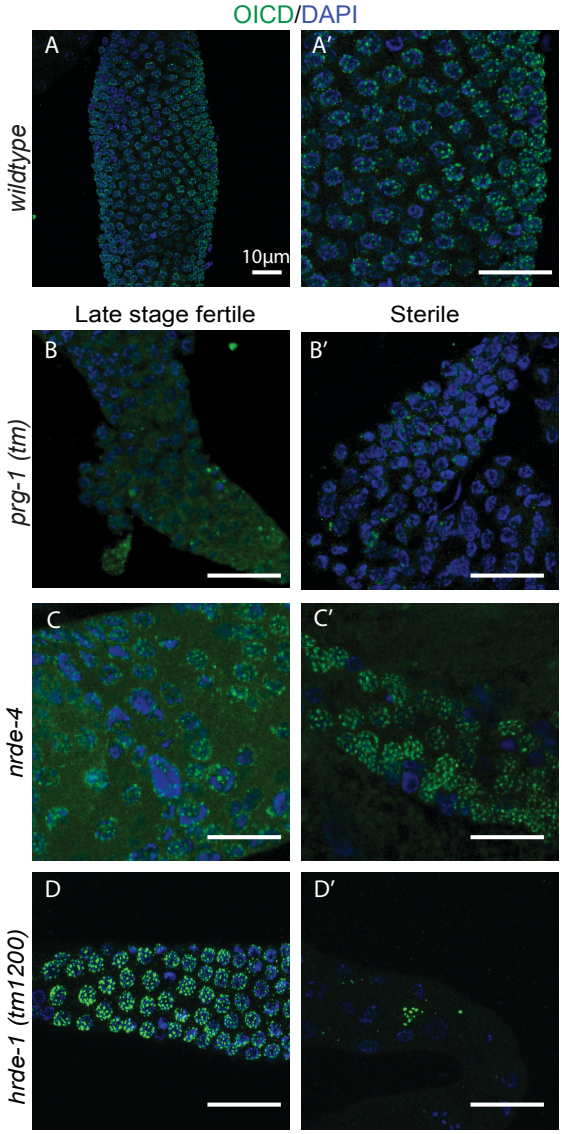

440

441 **Supplemental Figure 1: P-granule defects in *prg-1(tm), nrde- 4* and *hrde-1*.** Germlines of sterile

442 Day 2-3 adult animals were stained using the OIC1D4 antibody against P-granules (green) and

443 DAPI (blue). **(A-A')** Control animals contain uniform puncta of P-granule staining surrounding

444 each nuclei. **(B-D)** Late generation fertile *prg-1(tm), nrde-4*, and *hrde-1* animals displayed

445 relatively normal P-granule staining in the germlines. **(B'-D')** sterile *prg-1(tm), nrde-4*, and *hrde-*

446 *1* germ cell P-granules.

447

Genotype	Normal	Loss (>20%)	p-value
N2	32	0	
hrde-1 (tm1200)	0	31	<.0001
rsd-6 (yp11)	0	32	<.0001
nrde-2(gg95)	0	25	<.0001
rbr-2 (tm1231)	0	32	<.0001

448 **Table 1: Quantification of P-granule defects in the germline**

449